Fetal Diagnosis and Therapy

Fetal Diagn Ther 2008;24:203–210
DOI: 10.1159/000151339

Received: April 17, 2007
Accepted: June 22, 2007
Published online: August 28, 2008

In vivo Intrauterine Sound Pressure and Temperature Measurements during Magnetic Resonance Imaging (1.5 T) in Pregnant Ewes

E. Ruckhäberle[a] S.G. Nekolla[b] C. Ganter[c] K.T.M. Schneider[a] A. Peter[h] A. Raidt[d] L. Kovacs[e] S.J. Brockmeier[f] M. Schwaiger[b] R. Oberhoffer[g] N.A. Papadopulos[e]

Departments of [a]Perinatal Medicine, [b]Nuclear Medicine, [c]Radiology, [d]Experimental Surgery, and [e]Plastic and Reconstructive Surgery, [f]Section of Phoniatrics and Pedaudiology, Department of Otolaryngology, Klinikum rechts der Isar, Technical University Munich, [g]Department of Paediatric Cardiology, Kinderklinik Schwabing, Technical University Munich, Munich, [h]Department of Electrical Engineering, HTW University of Applied Sciences Dresden, Dresden, Germany

Key Words

Amniotic fluid · Intrauterine sound pressure · Fetal auditory system · Magnetic resonance imaging · Radiofrequency energy · Specific absorption rate

Abstract

Objective: To investigate the influence of several magnetic resonance imaging (MRI) sequences on amniotic fluid temperature and intrauterine sound pressure. ***Material and Methods:*** Temperature and sound pressure measurements during MRI (1.5 T) in pregnant ewes were done. Linear levels and third octave band spectra were compared. ***Results:*** No significant changes in the temperature of amniotic fluid were observed. Intrauterine summation levels reached peak levels up to 103.0 dB(A) before starting the MRI sequence and levels up to 116.0 dB(A) during a real-time sequence. Evaluating the octave band spectra, peak levels did not exceed 100.0 dB(L). ***Conclusions:*** Our delimited data revealed no harm for the fetus by an increase in amniotic fluid temperature or hazards for the fetal auditory system by different MRI sequences.

Introduction

Although B-mode and Doppler ultrasound imaging are the most commonly used techniques in prenatal diagnosis, disadvantages like low tissue contrast and differentiation have resulted in the use of new applications and techniques. Favorable characteristics such as missing radiation exposure, high detail accuracy, possibility of volume imaging and low inter- and intraobserver variability have resulted in a wider use of magnetic resonance imaging (MRI) in obstetrical diagnosis [1–5].

Because of these advantages, MRI gains scientific interest in pre-, peri- and postnatal diagnosis both for fetal as well as maternal imaging [1, 5–7].

Echocardiography is the clinical mainstay in assessment of the fetal heart; however, it is not a true three-dimensional imaging modality and can be constrained by acoustic windows [8, 9, 11]. To overcome these problems, MRI has been increasingly used in prenatal structural evaluation of abnormalities of the fetal heart beginning in the late 1990s. This was enabled by new techniques like rapid imaging, real-time sequences, velocity mapping

KARGER

Fax +41 61 306 12 34
E-Mail karger@karger.ch
www.karger.com

1015–3837/08/0243–0203$24.50/0

Accessible online at:
www.karger.com/fdt

PD Dr. med. Nikolaos A. Papadopulos, MD
Department of Plastic and Reconstructive Surgery
Klinikum rechts der Isar, Technical University Munich
Ismanninger Strasse 22, DE–81675 Munich (Germany)
Tel. +49 89 4140 2171, Fax +49 69 4140 4869, E-Mail n.papadopulos@lrz.tum.de

and angiography [10–13]. Recently, even functional MRI evaluation of the fetal heart has been described [12].

However, before these advances and new techniques of MRI can be routinely used in obstetrical diagnosis, a reevaluation of safety aspects, in particular increase in amniotic fluid temperature and the effect on fetal hearing is essential.

Although former investigations found no significant increase in the temperature of the amniotic fluid with HASTE sequences [14, 15], these results had to be approved for real-time sequences.

There exists some but not much consolidated knowledge about fetal hearing.

We aimed to investigate the influence of several MRI sequences, especially real-time sequences, on amniotic fluid temperature and intrauterine sound pressure levels. Within this experimental setup, a risk calculation for further use of MRI in fetal diagnosis was the target of the presented study. To achieve this, we performed intrauterine temperature and acoustic measurements at three different imaging sequences using an animal model.

Material and Methods

Animal Studies

For our experiments we used the sheep model, which is a well-established animal model in intrauterine surgery. Our objective was to measure temperature and sound pressure levels inside and outside the uterus. The comparison of external and intrauterine levels allows an estimate of possible attenuation of levels throughout the abdominal walls. An additional comparison of an intrauterine measurement without and with running MRI sequences should not only assess the 'background noise level' inside the uterus but also highlight the 'real' influence of the particular sequence on the intrauterine pressure levels. The comparison of the octave bands of sound with and without MRI sequence has the potential to approximate risk estimation for fetal hearing.

After ethical approval by the Technical University Munich and the Bavarian Government, pregnant ewes at a gestational age of 120 days were anesthetized [for details on the anesthesia, see 16, 17]. After laparotomy and hysterotomy, a hydrophone (Type 8103; Brüel & Kjaer®, Naerum, Denmark) and a temperature sensor (T430–4L; AMR®, Holzkirchen, Germany) were introduced into the uterus and placed near the fetal ear. The dimensions of the hydrophone are as follows: length = 50 mm, diameter = 9.5 mm and an attached shielded Teflon cable with a length of 3 m.

After closure of the abdominal walls and bedding of the narcotized ewe into the MRI tomograph (Sonata™, B = 1.5 T, Siemens Medical Solutions, Erlangen, Germany) the readings started. Overall, two measurements with two different ewes on two different days were carried out.

We measured external and intrauterine sound pressure levels before starting the imaging of the MRI system (background reference) and during three different MRI sequences. Reference recording without MRI sequence was performed to estimate the amount of background noise level, composed of bowel movements, respiratory and cardiac activity.

In parallel to the intrauterine readings, external temperature was measured using a temperature sensor T430-4L (AMR) in combination with the ALMEMO 2290-8 system (AMR). Data storing and triggering of the internal and external temperature measurements were controlled with the acquisition program AMR Win Control™ V3.3.0 (AMR). Due to interferences between the Ni-Cr temperature sensor and the magnetic field, we were able to measure temperature only before and after imaging for 2 min, while sound pressure was measured during the sequence.

External sound pressure levels were recorded by a condenser microphone (type 4190; Brüel & Kjaer). The two signals of the hydrophone and the microphone were amplified by a 2-channel microphone amplifier (type 2669L, Brüel & Kjaer) and finally dubbed to, and postprocessed by the signal analyzer system Pulse 3560C (Brüel & Kjaer). The filter of the amplifier was set to f_l = 50 Hz and f_u = 6.4 kHz. All sound pressure levels were referenced to the reference pressure p_0 = 20 μPa.

Out of the absolute levels, equivalent continuous sound levels are A-weighted [L_{eq}(A)] and calculated by the measurement system Pulse 3560C (Brüel & Kjaer). The system measured the complete third band spectra of A-weighted and linear (L) sound pressure levels L_p.

The measure system was calibrated before and after each measurement with a piston phone (Sound Level Calibrator Type 4231, Brüel & Kjaer) to an L_p of 94 dB by a frequency of 1 kHz.

Magnetic Resonance Imaging

We selected three imaging sequences with distinct differences: the HASTE whisper sequence was optimized for morphological imaging while minimizing the acoustical effects of gradient switching in order to provide a maximum of patient comfort. The second sequence was a fast HASTE sequence with reduced sensitivity of motion artifacts while also focusing on morphological imaging. Finally, an ultra-fast real-time true FISP imaging sequence was used for imaging of moving structures in the fetus, (e.g. the heart as no direct ECG signal of the fetus is available). However, such a trigger signal is mandatory in conventional cardiovascular MR imaging as otherwise severe motion artifacts are observed. Thus, a nontriggered, real-time sequence might provide an approach in such a setting.

The technical parameters of all three sequences are summarized in table 1.

Results

In the temperature measurements, we found a decrease in intrauterine temperature between measurement before (38.18°C) and after one sequence (38.21°C; see fig. 4). The observation of the temperature over the course of measuring from the beginning of our experiment (38.18°C) until the end after the third sequence (38.27°C; fig. 1b) had shown essentially no increase. The ΔT of

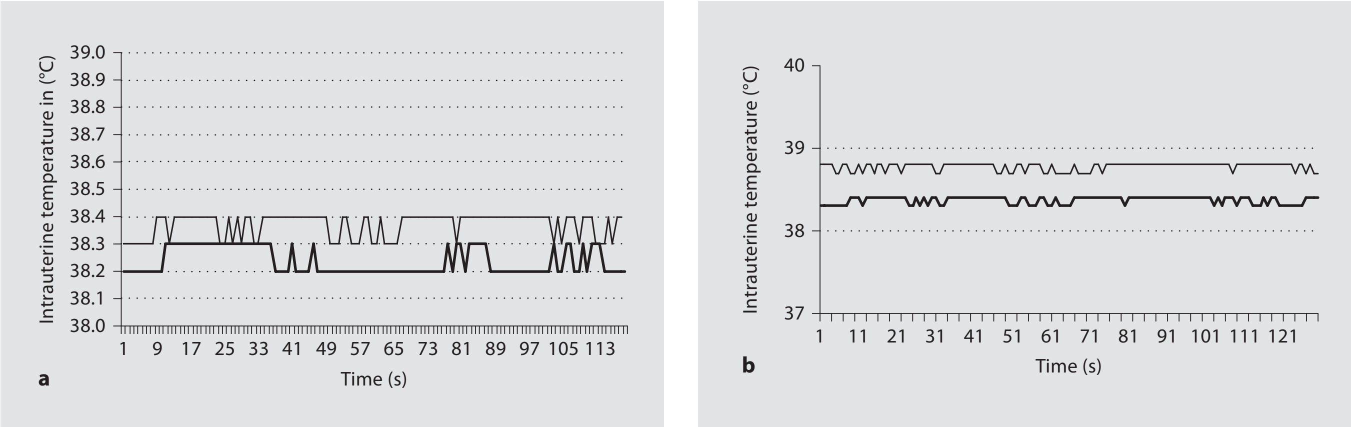

Fig. 1. a Temperature-time diagram of the intrauterine temperature before (thick line) and after the HASTE whisper MRI sequence (thin line). **b** Temperature-time diagram of the intrauterine temperature before (thick line) and after all three MRI sequences consecutively (thin line).

Table 1. Summary of the imaging parameters of the three used sequences

Sequence	TR ms	TE ms	Flip angle	ETL	Bandwidth Hz/pixel	Slice thick-ness, mm	Field of view mm × mm	Matrix
HASTE whisper	n/a	83	90°	143	130	4	400 × 400	143 × 256
HASTE fast	n/a	75	90°	143	130	4	400 × 400	143 × 256
True FISP real-time	2.5	1.1	40°	n/a	1,345	10	400 × 400	79 × 128

0.09 K is in the measuring tolerance of the device and seems to be a quantization deviation [18].

Intrauterine peak (L_{max}) levels were 106.0 dB(A) for the HASTE whisper, 110.0 dB(A) for the HASTE fast and 116.0 dB(A) for the real-time true FISP sequence. In neither case were external levels higher than intrauterine levels (fig. 2).

In addition to comparisons of external and intrauterine levels, an assessment of the ratio between normal intrauterine background sound and the amount of intrauterine sound during the different MRI sequences was made.

Within the reference recording before running sequence, a fairly homogenous sound with intrauterine L_{max} levels of up 103 dB(L) and external L_{max} levels of 62 dB(L) were recorded (fig. 2). Third octave band analysis of these intrauterine hydrophone recordings showed only in the very low frequency area below 63 Hz higher L_{max} levels up to 97 dB(L). This might be explained by the frequency of alternating current of the power supply system (50 Hz). For higher frequencies, L_{max} levels did not exceed 85 dB(L).

In the comparison of summation pressure levels before and in run time of the sequence, we observed ΔL of 3 dB(L) for HASTE whisper, ΔL of 7 dB(L) for HASTE fast and ΔL of 13 dB(L) for true FISP inside the uterus, while external recordings yielded ΔL of 28 dB(L) for HASTE whisper, ΔL of 40 dB(L) for HASTE fast and ΔL of 38 dB(L) for true FISP (fig. 3a, 4a, 5a).

Apart from summation pressure levels, we investigated third octave bands of internal and external recordings and compared these recordings with measurements before the MRI sequences (fig. 3b, 4b, 5b).

Analysis of the third octave band of these recordings resulted in highest differences (ΔL = 28 dB) in the low-frequency bands (between 100 and 200 Hz) for the HASTE sequences. The highest differences (ΔL = 34 dB) were observed in the frequency bands from 250 to 4,000 Hz for the true FISP sequence.

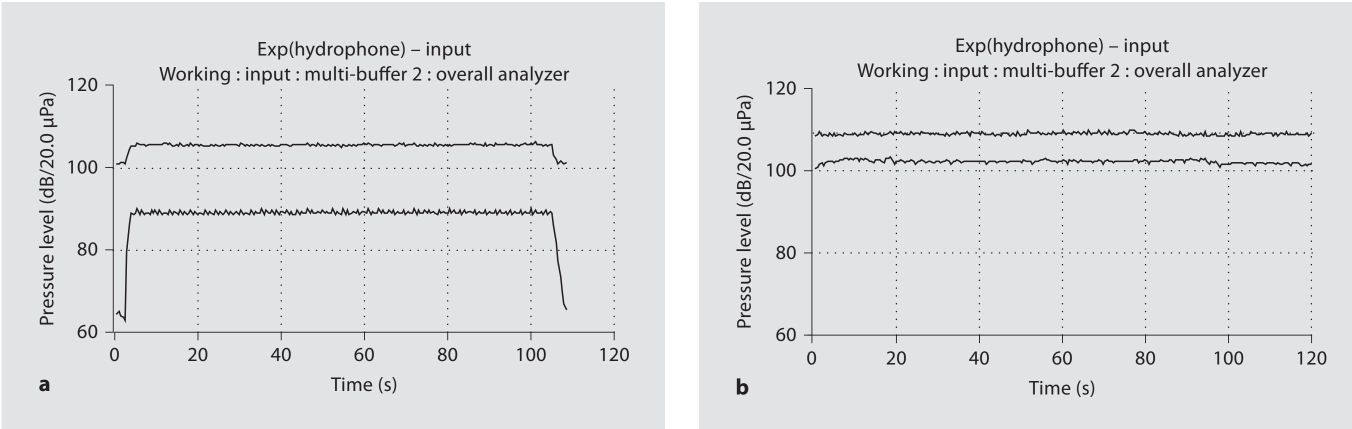

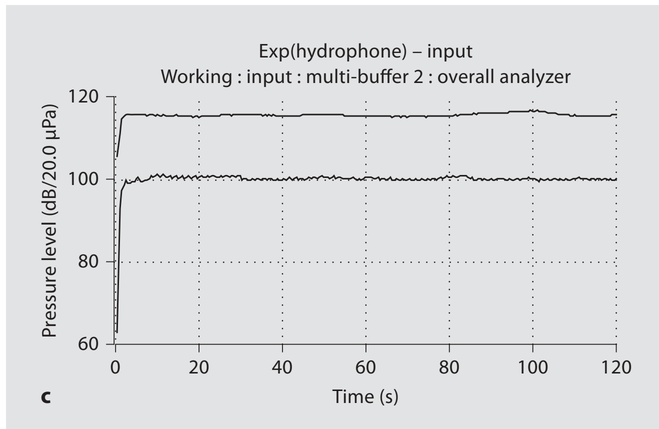

Fig. 2. Pressure level (linear weighted)-time diagram of the external microphone recordings (lower tracing) and the intrauterine hydrophone recording (upper tracing) for three MRI sequences. **a** HASTE whisper; note the switch on/switch off phenomenon of the MRI sequence. **b** HASTE fast. **c** True FISP.

Evaluating the third octave band frequency, dependent peak levels were mostly found at f_m = 50, 800 and 1,600 Hz.

For the HASTE whisper and the HASTE fast sequence, intrauterine L_p levels never exceeded 100 dB in an f_m below 500 Hz (fig. 3b, 4b). Frequency-dependent peak levels in the frequency band below 500 Hz were L_p (100 Hz) = 95 dB(L) and L_p (50 Hz) = 99 dB(L) for the HASTE whisper and L_p (100 Hz) = 92 dB(L) and L_p (50 Hz) = 98 dB(L) for the HASTE fast.

Intrauterine levels were lower in the real-time sequence compared with the two other sequences in the critical f_m band below 500 Hz. Reached L_p levels were 98 dB at an f_m of 500 Hz (fig. 5b). For the higher f_m above 1 kHz, intrauterine L_p levels exceeded 100 dB with a maximum L_p of 110 dB at an f_m of 2 kHz.

Analysis of the pressure level difference in the frequency band from 63 to 250 Hz has shown little variation between reference recording and recording during the real-time sequence. A ΔL of 22 dB(L) was recorded for the HASTE sequences. In the frequency band from 250 to 1,000 Hz, ΔL grew up to 25 dB(L) for the HASTE and more than 30 dB(L) for the true FISP sequence.

Discussion

The objective of our experiments was to re-evaluate risks of different MRI sequences on intrauterine amniotic fluid temperature and on fetal hearing. To our knowledge, this is the first report of an animal experiment about the influence of real-time MRI on amniotic fluid temperature and intrauterine sound pressure level.

Our investigation suggests that there is no risk for the unborn by the increase in the amniotic fluid temperature throughout fast MRI sequences. Some of these sequences induce high intrauterine sound pressure levels. If intrauterine summation levels for all three sequences exceeded 100 dB(L), the third octave band levels did not exceed 100 dB for these sequences. Those frequency-dependent

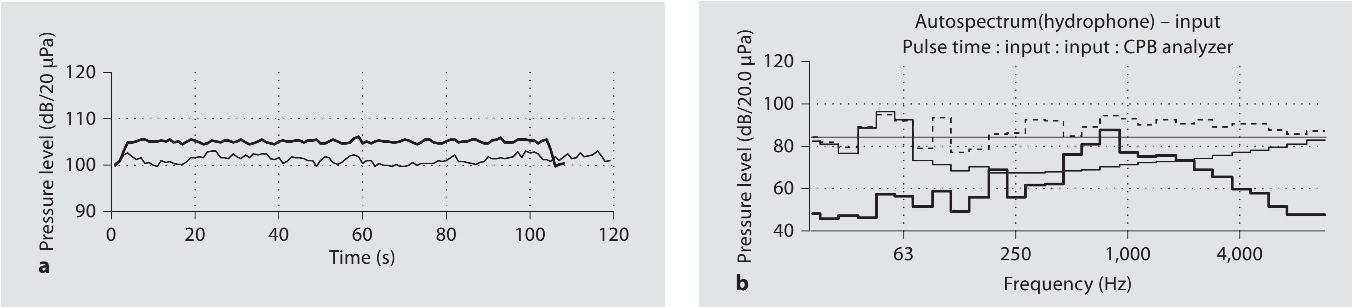

Fig. 3. a Pressure level (L weighted)-time diagram of a HASTE whisper sequence (thick line) and a recording without MRI sequence (thin line). Recording started before switching on the MRI unit (displayed by an increase at the beginning and the drop at the end of the curve). **b** Third octave band analysis of the external microphone recording (thick line) and hydrophone recording in the uterus during the HASTE whisper sequence (dashed thin line) in comparison with a reference recording before running the MRI sequence (thin line). The high pressure levels in the frequency band below 63 Hz might be explained by the power frequency of the alternating current at 50 Hz. Cursor value of the measurement software (thin straight line).

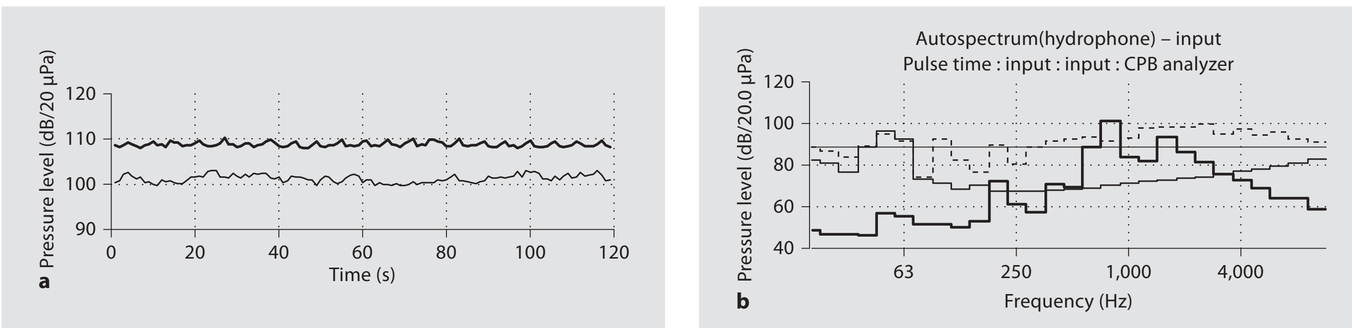

Fig. 4. a Pressure level (L weighted)-time diagram of a HASTE fast sequence (thick line) and a recording without MRI sequence (thin line). **b** Third octave band analysis of the external microphone recording (thick line) and hydrophone recording inside the uterus during the HASTE fast sequence (dashed thin line) in comparison with a reference recording before running the MRI sequence (thin line). Cursor value of the measurement software (thin straight line).

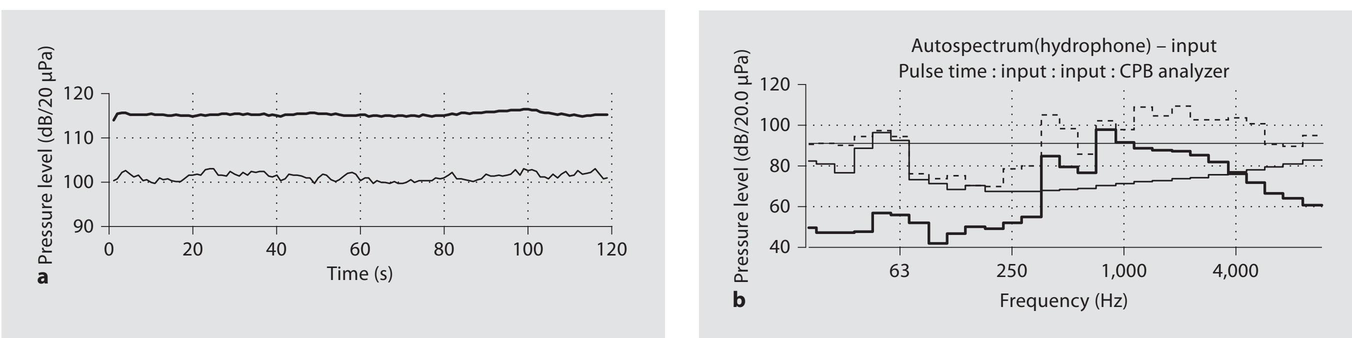

Fig. 5. a Pressure level (L weighted)-time diagram of a true FISP sequence (thick line) and a recording without MRI sequence (thin line). **b** Third octave band analysis of the external microphone recording (thick line) and hydrophone recording in the uterus during the true FISP sequence (dashed thin line) in comparison with a reference recording before running the MRI sequence (thin line). Cursor value of the measurement software (thin straight line).

levels are more important for risk assessment. Additionally, the risk for the fetus seems to be low because of attenuation of $\Delta L = 10–15$ dB by sound conduction to the fetal inner ear for the critical low-frequency energy ($f < 500$ Hz; [19]). However, a strict indication and limitation of fetal MRI examinations should be demanded. Follow-up evaluation after delivery failed to show any negative influence of MRI on newborn's hearing.

MRI has the big advantage of nonionising radiation exposure to mother or child, and has been shown to have no teratogenic or mutagenic effects on the fetus [1, 2].

MRI uses three components for image generation from inside the body, a static magnetic field, pulsed radiofrequency and time-varying gradient electromagnetic fields. The hazard associated with radiofrequency energy is heating of the amniotic fluid or uterine structures. Edwards et al. [20] reviewed the effects of heat on embryo and fetus. Little information is given about hazards for the fetus by heating effects by short periods of MRI exposure. Our experiments confirm the results of Levine et al. [15] and Kawabata et al. [14] who found no risk of an increase in amniotic fluid temperature throughout fast MRI sequences. The observed difference in temperature of 0.09 K between the beginning of our experiment and the end (time range, 1 h) is in the normal range of the measuring device and is most likely a quantization deviation. This result is in full agreement with the existing international standard for MRI systems (IEC 60601-2-33: 2006-02: Medical electrical equipment – part 2-33: Particular requirements for the safety of magnetic resonance equipment for medical diagnosis).

To ensure that these values are met, the specific absorption rates (SARs) are set before the imaging starts [21]. Here, we would like to point out the results of Hand et al. [21] who found for the fetus in part explicitly higher levels for the local SAR compared to the SAR of the body. Still, we cannot say how far these results influence the fetus in vivo.

A second major concern is the acoustic noise generated in the MRI system and its effects on the fetal auditory system. The noise results from the rapid switching of the electrical currents within the gradient coils. This, combined with the presence of a strong magnetic field, produces significant Lorentz forces. These forces make the coils vibrate producing a loud knocking noise.

Sound pressure levels measured by external reference microphone are in agreement with the results of Shellock et al. [22] who used same field strength of $B = 1.5$ T. Looking at only the linear sound pressure levels, L_p up to 116 dB(L) were observed during real-time sequences. The somewhat lower levels recorded by the external microphone are due to the distance of the microphone to the coil. This distance had to be kept because of the electrostatic attraction of the ferromagnetic parts of the microphone towards the magnet.

As described by Gerhardt and Abrams [23], two factors influence the stimuli that evoke response from the fetus – first, the attenuation for different frequencies that is provided by the tissues and fluids surrounding the fetus, and second the transmission of sound from the fluid around the head to the inner ear [24].

In contrast to other authors [25], we could not observe directly an intrauterine attenuation of sound from the external to intrauterine recordings. Aware of the difference between microphone and hydrophone recordings, we measured the deviations between the reference recording before and during MRI. The obvious larger differences in external recordings confirm the results of other reports [19, 24–26] of an attenuation of sound by maternal tissues. Other authors [27–29] report of dependence of intra-abdominal levels on stimulus frequency and intra-abdominal location of the fetal ear. Abdominal wall enhances low-frequency sound of $f_m < 200$ Hz by $\Delta L < 5$ dB and attenuates higher-frequency sound by up to 20 dB [23, 26, 28].

Secondly, as mentioned above, the fetal hearing is affected by the transmission of the sound from the fluid at the fetal head into the inner ear. An important fact in this context is the sound environment of the fetus. Consistent with other authors [30–32], sounds generated inside the mother ('noise floor') can reach L_{max} levels up to 103 dB(A). According to the current model of fetal hearing [23], extrinsic sounds have to exceed 'noise level' in order to be detected by the fetus. Gerhardt et al. [24] and Huang et al. [33] found in their experiments with cochlear microphones in lambs an attenuation of 10–15 dB for low-frequency energy and an attenuation of 40–50 dB for high-frequency energy ($f_m > 0.5$ kHz). Interestingly, for the HASTE sequences differences in the low frequency area reach 28 dB(L). This implies a higher influence on fetal hearing, whereas differences in the real-time sequences were only modest. Taking the reported attenuation into consideration, for all three sequences the risk of damage to the fetal auditory system is low.

The Committee of Hearing, Bioacoustics and Biomechanics of the US Department of Labor recommended avoidance of sound pressure levels (L_{gr}) of 90 dB(A) to pregnant women for extended periods of time [22]. To our knowledge there are no explicit recommendations for noise exposure of fetuses, however we used an L_{gr} of 90 dB(A) as a guideline level.

The final aspect of our examination was the impairment of mother's hearing due to the MRI. Taking into consideration external L_p levels up to 102 dB(L) in our measurements and the results of Radomskij et al. [34] and McJury and Shellock [35], who found a potential hearing impairment by high sound pressure levels in MRI. Thus, good ear protection and short-lasting examination times are mandatory.

In conclusion, there is no risk to the unborn from increased amniotic fluid temperature. MRI sequences induce, in part, high intrauterine sound pressure levels. Intrauterine summation levels for all sequences exceeded an L_{gr} of 100 dB(L). Nevertheless, harm to the fetus seems implausible due to lower unweighted levels and differences in the low-frequency band and the reported attenuation of 10–15 dB by sound conduction to the fetal inner ear.

Our small data of auditory follow-up evaluation in human neonates failed to show any negative influence of MRI on newborn's hearing. A hazard to the fetus is highly implausible, but cannot be completely excluded. Thus, strict indications for fetal MRI are necessary.

Acknowledgments

Our special thanks go to the companies Brüel & Kjaer and AMR, which provided the described instruments and put maintenance and calibration into practice. Without their assistance none of our experiments would have been made possible. We would like to express our special gratitude to Mr. Schuh from Brüel & Kjaer. He made our readings possible and helped us with the analysis and interpretation of our results. Additionally, we would like to thank Mr Hüttl from AMR who provided us with the necessary information about the measurement tool and the interpretation of our results of the temperature measurements.

References

1 De Wilde JP, Rivers AW, Price DL: A review of the current use of magnetic resonance imaging in pregnancy and safety implications for the fetus. Prog Biophys Mol Biol 2005;87: 335–353.
2 Formica D, Silvestri S: Biological effects of exposure to magnetic resonance imaging: an overview. Biomed Eng Online 2004;3:11.
3 Levine D, Barnes PD, Sher S, Semelka RC, Li W, McArdle CR et al: Fetal fast MR imaging: reproducibility, technical quality, and conspicuity of anatomy. Radiology 1998;206: 549–554.
4 Levine D, Barnes PD, Robertson RR, Wong G, Mehta TS: Fast MR imaging of fetal central nervous system abnormalities. Radiology 2003;229:51–61.
5 Levine D: Fetal magnetic resonance imaging. J Matern Fetal Neonatal Med 2004;15: 85–94.
6 Sandrasegaran K, Lall C, Aisen AA, Rajesh A, Cohen MD: Fast fetal magnetic resonance imaging. J Comput Assist Tomogr 2005;29: 487–498.
7 Zaretsky MV, Alexander JM, McIntire DD, Hatab MR, Twickler DM, Leveno KJ: Magnetic resonance imaging pelvimetry and the prediction of labor dystocia. Obstet Gynecol 2005;106:919–926.
8 Deng J, Brookes JA, Gardener JE, Rodeck CH, Lees WR: Three-dimensional magnetic resonance imaging of the postmortem fetal heart. Fetal Diagn Ther 1996;11:417–421.
9 Deng J, Rodeck CH: New fetal cardiac imaging techniques. Prenat Diagn 2004;24:1092–1103.
10 Fogel MA, Weinberg PM, Haselgrove J: Nonuniform flow dynamics in the aorta of normal children: a simplified approach to measurement using magnetic resonance velocity mapping. J Magn Reson Imaging 2002;15: 672–678.
11 Budorick NE, Millman SL: New modalities for imaging the fetal heart. Semin Perinatol 2000;24:352–359.
12 Fogel MA, Wilson RD, Flake A, Johnson M, Cohen D, McNeal G, et al: Preliminary investigations into a new method of functional assessment of the fetal heart using a novel application of 'real-time' cardiac magnetic resonance imaging. Fetal Diagn Ther 2005; 20:475–480.
13 Lee VS, Resnick D, Bundy JM, Simonetti OP, Lee P, Weinreb JC: Cardiac function: MR evaluation in one breath hold with real-time true fast imaging with steady-state precession. Radiology 2002;222:835–842.
14 Kawabata I, Takahashi Y, Iwagaki S, Tamaya T: MRI during pregnancy. J Perinat Med 2003;31:449–458.
15 Levine D, Zuo C, Faro CB, Chen Q: Potential heating effect in the gravid uterus during MR HASTE imaging. J Magn Reson Imaging 2001;13:856–861.
16 Papadopulos NA, Zeilhofer HF, Papadopoulos MA, Feussner H, Henke J, Kovacs L, et al: Experimental endoscopic intrauterine surgery for craniofacial malformations such as the cleft lip and palate (in German). Mund Kiefer Gesichtschir 2003;7:70–75.
17 Papadopulos NA, Papadopoulos MA, Zeilhofer HF, Boos H, Henke J, Erhardt W et al: Intrauterine autogenous foetal bone transplantation for the repair of cleft-like defects in the mid-gestational sheep model. J Craniomaxillofac Surg 2004;32:199–210.
18 Bernhard F: Thermocouples; in Bernhard F (ed): Technical Temperature Measurement, ed 1. Berlin, Springer, 2004, pp 768–772.
19 Gerhardt KJ, Pierson LL, Huang X, Abrams RM, Rarey KE: Effects of intense noise exposure on fetal sheep auditory brain stem response and inner ear histology. Ear Hear 1999;20:21–32.
20 Edwards MJ, Saunders RD, Shiota K: Effects of heat on embryos and foetuses. Int J Hyperthermia 2003;19:295–324.
21 Hand JW, Li Y, Thomas EL, Rutherford MA, Hajnal JV: Prediction of specific absorption rate in mother and fetus associated with MRI examinations during pregnancy. Magn Reson Med 2006;55:883–893.
22 Shellock FG, Ziarati M, Atkinson D, Chen DY: Determination of gradient magnetic field-induced acoustic noise associated with the use of echo planar and three-dimensional, fast spin echo techniques. J Magn Reson Imaging 1998;8:1154–1157.
23 Gerhardt KJ, Abrams RM: Fetal exposures to sound and vibroacoustic stimulation. J Perinatol 2000;20:S21–S30.
24 Gerhardt KJ, Huang X, Arrington KE, Meixner K, Abrams RM, Antonelli PJ: Fetal sheep in utero hear through bone conduction. Am J Otolaryngol 1996;17:374–379.

25 Glover P, Hykin J, Gowland P, Wright J, Johnson I, Mansfield P: An assessment of the intrauterine sound intensity level during obstetric echo-planar magnetic resonance imaging. Br J Radiol 1995;68:1090–1094.
26 Abrams R, Gerhardt K, Antonelli P: Fetal hearing. Dev Psychobiol 1998;33:1–3.
27 Gerhardt KJ, Abrams RM: Fetal hearing: characterization of the stimulus and response. Semin Perinatol 1996;20:11–20.
28 Peters AJ, Gerhardt KJ, Abrams RM, Longmate JA: Three-dimensional intraabdominal sound pressures in sheep produced by airborne stimuli. Am J Obstet Gynecol 1993;169:1304–1315.
29 Gerhardt KJ, Abrams RM, Huang X, Griffiths SK, Peters AJ: Intra-abdominal sound pressure levels during impulse noise exposure in sheep. Mil Med 2000;165:153–156.
30 Abrams RM, Gerhardt KJ: The acoustic environment and physiological responses of the fetus. J Perinatol 2000;20:S31–S36.
31 Armitage SE, Baldwin BA, Vince MA: The fetal sound environment of sheep. Science 1980;208:1173–1174.
32 Gerhardt KJ, Abrams RM, Oliver CC: Sound environment of the fetal sheep. Am J Obstet Gynecol 1990;162:282–287.
33 Huang X, Gerhardt KJ, Abrams RM, Antonelli PJ: Temporary threshold shifts induced by low-pass and high-pass filtered noises in fetal sheep in utero. Hear Res 1997;113:173–181.
34 Radomskij P, Schmidt MA, Heron CW, Prasher D: Effect of MRI noise on cochlear function. Lancet 2002;359:1485.
35 McJury M, Shellock FG: Auditory noise associated with MR procedures: a review. J Magn Reson Imaging 2000;12:37–45.